Jet structure and variability studies of GRBs with 3D GRMHD simulations of magnetically arrested disks

Bestin James, Agnieszka Janiuk, Fatemeh Hossein Nouri

Center for Theoretical Physics PAS, Warsaw

8th Conference of the Polish Society on Relativity, September 20, 2022, Warsaw

Gamma Ray Bursts

- Gamma Ray Bursts (GRBs) - most energetic events observed in the universe, releasing a total energy of upto 10^{52}-10^{54} erg/s.
- Two classes of GRBs - based on their duration: short and long GRBs
  - Short GRBs: a few ms to < 2 s
  - Long GRBs: > 2 s to a few hundred seconds
- Typically, different mechanisms explaining their central engines
  - BH-NS or BNS merger for short-GRBs
  - Collapsar scenario for long-GRBs
- Both scenarios can result in an accretion disk around a central black hole.

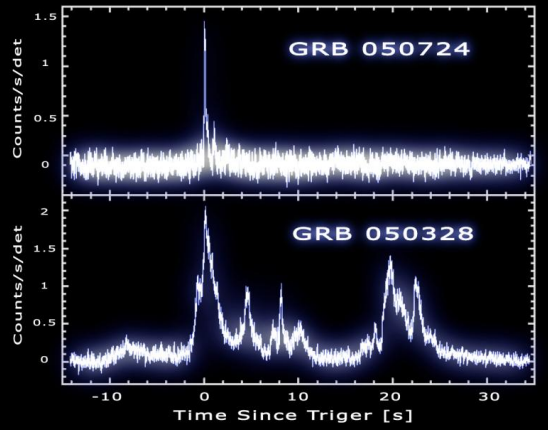

Image Credits: Top: Artist's impression of a GRB - ESO/A. Roquette
Bottom: Light curves of short and long GRBs - NASA

Gamma Ray Bursts

- GRBs show very fast variability in time which goes up to ms scales.
- They show complex jet structures rather than a simple top hat, as was initially assumed.
- Jet opening angles span over a wide range of values from a few degrees to over 30 or more.
- The reasons for the origin of high energy emission are not clear.
- Generally have large-scale magnetic fields in their central engines which affect their dynamic nature.

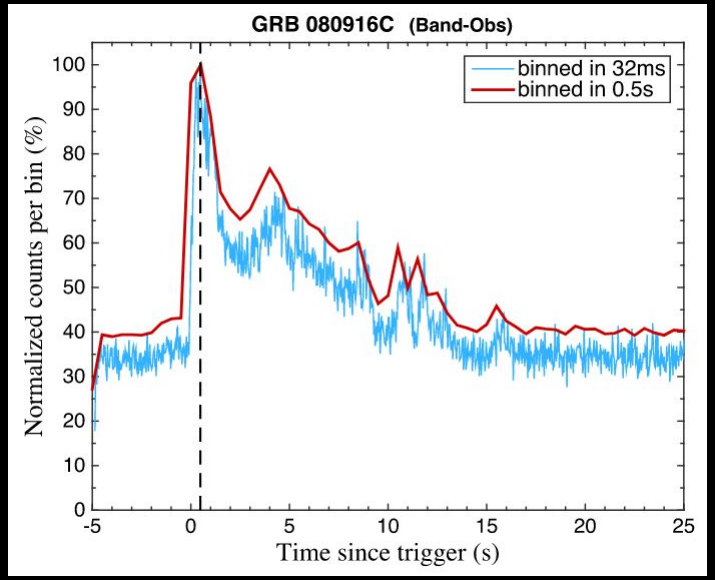

An example light curve of a GRB with sub-second variability: The light curve in the 20–200 keV band of GRB 080916C.

Credit: Yue Liu et al. 2018

Relativistic Jets

- GRBs are observed as relativistic jets pointing towards our line of sight.
- Such jets are Poynting-dominated, plausibly powered by the Blandford & Znajek (1977) mechanism which can extract rotational energy from a black hole

$$P_{BZ} \sim \frac{\phi_{BH}^2 \cdot \Omega_{BH}^2}{c}$$

- The properties of the central engine might affect the jet properties.
- We investigate this with our 3D GRMHD simulations of accretion disks and the associated jet base in a fixed Kerr geometry.

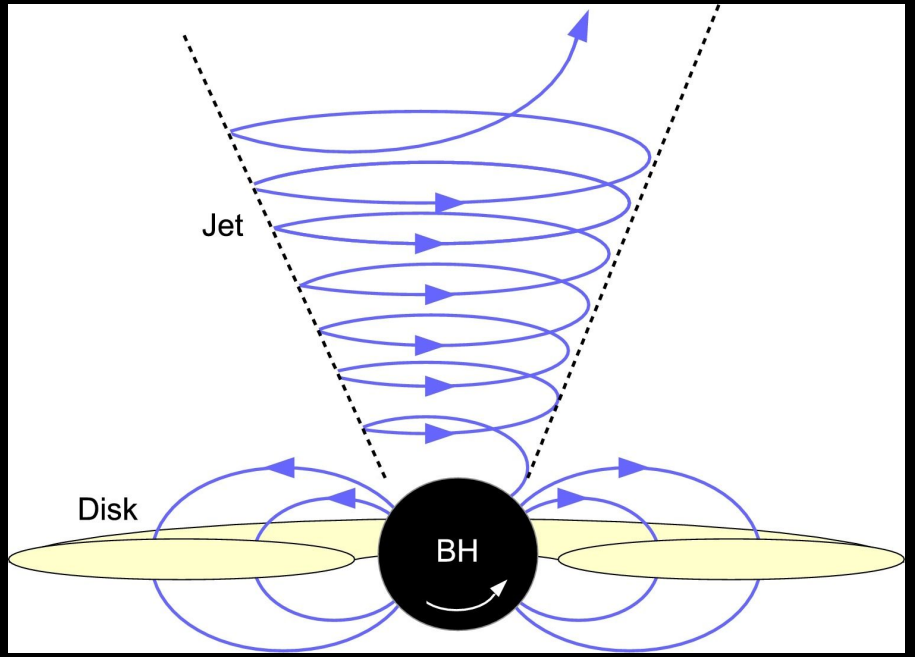

Relativistic jet launching from a black hole-accretion disk system, through the Blandford-Znajek mechanism. Magnetic field lines (blue) are anchored in the accretion disk (yellow) and penetrate the black hole's ergosphere. Spinning BH twists open field lines, leading to a jet.

Credit: V. Takhistov, 2018

HARM code

We use the HARM code, a conservative, shock capturing scheme, for evolving the equations of GRMHD, originally developed by Gammie et al. (2003).

The code provides a solver for the continuity, energy-momentum conservation and induction equations in GR:

$$\nabla_\mu(\rho u^\mu) = 0; \nabla_\mu(T^{\mu\nu}) = 0; \nabla_\mu(u^\nu b^\mu - u^\mu b^\nu) = 0$$

The stress-energy tensor, in general, contains the gas and electromagnetic parts:

$$T^{\mu\nu} = T^{\mu\nu}_{gas} + T^{\mu\nu}_{EM}$$

$$T^{\mu\nu}_{gas} = \rho h u^\mu u^\nu + p g^{\mu\nu} = (\rho + u + p) u^\mu u^\nu + p g^{\mu\nu}$$

$$T^{\mu\nu}_{EM} = b^2 u^\mu u^\nu + \frac{1}{2} b^2 g^{\mu\nu} - b^\mu b^\nu; b^\mu = u^*_\nu F^{\mu\nu}$$

where u is internal energy, u^μ is four-velocity of gas, and $b^\mu = ½\varepsilon^{\mu\nu\rho\sigma} u_\nu F_{\rho\sigma}$.
In force-free approximation, $E_\nu = u_\mu F^{\mu\nu} = 0$. The code works in the natural unit convention with G=c=M=1.

Plasma Instabilities Involved

- Magnetorotational Instability (MRI):
  - Originally described by Velikov (1959) and Chandrasekhar (1960).
  - Importance to accretion disks was recognized by Balbus & Hawley (1991).
- Interchange instability:
  - Driven by gradients in magnetic pressure in plasma in the areas where the confining magnetic field is curved.
  - The name refers to the action of the plasma changing position with the magnetic field lines without significant disturbance to the geometry of the external field.

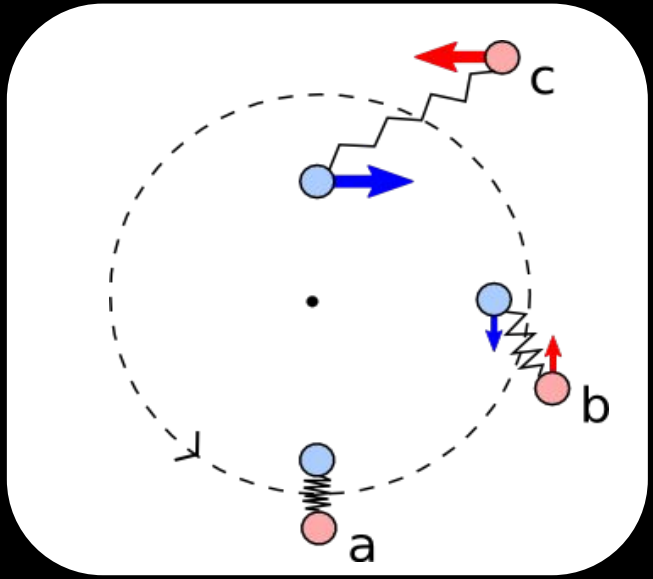

A simple toy model for MRI. Two small masses connected by a spring orbiting a central mass. In highly conductive plasmas, the magnetic field acts as the spring, giving rise to magnetorotational instability.

Image credit: Nick Murphy, Harvard-CfA

Numerical Setup

- We explore the scenario of magnetically driven accretion and jet variability related to the formation of **magnetically arrested accretion disk** state
- The initial conditions of our models assume the existence of a pressure equilibrium disk, embedded in a poloidal magnetic field.
- Disk initial configurations prescribed according to **Fishbone & Moncrief (1976) (FM76 model)** and **Chakrabarti (1985) (Ch85 model)** analytic solutions of equilibrium disks. They differ in the angular momentum distribution within the disk.
- In Ch85, the angular momentum distribution has a power law relation with the parameter $\lambda = (\ell/\Omega)^{1/2}$, where ℓ is the specific angular momentum and Ω is the angular velocity.

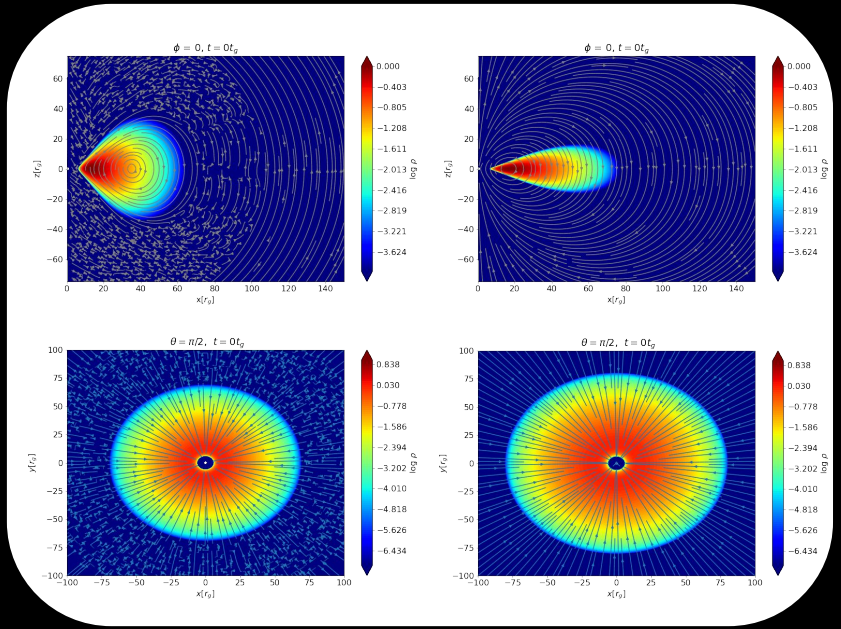

The initial disk structure in our 3D simulations for our two models. The plots show the density distribution at t = 0 t_g for the Fishbone-Moncrief (FM) initial condition (left panels) and the Chakrabarti initial condition (right panels) embedded in poloidal magnetic fields.

Numerical Setup

- We consider our FM76 model for the structure of a collapsar disk and Ch85 for the remnant of BNS merger.
- In the FM76 model - initial magnetic field is prescribed in such a way that the field lines follow the contours of density in disk.

$$A_\phi(r,\theta) = r^5(\rho_{avg}/\rho_{max}) - 0.2$$

- In the Ch85 model - the initial field is prescribed as the magnetic field produced by a circular current at r_{max}. The only non-zero component of the vector potential can be written as

$$A_\phi(r,\theta) = A_0 \frac{(2-k^2)K(k^2)-2E(k^2)}{k\sqrt{4Rr\sin\theta}}; k = \sqrt{\frac{4Rr\sin\theta}{r^2+R^2+2rR\sin\theta}}$$

with E and K the complete elliptic integrals, R the position of the circular current in the torus (same as r_{max} in our model) and A_0 a constant parameter.

Magnetically Arrested Disk

- The imposed poloidal magnetic fields results in the development of MRI and starts the accretion.
- The accreting plasma brings along with it more poloidal magnetic field to the black hole (BH) horizon.
- The magnetic flux accumulated on the black hole horizon (normalized to mass flux) can be quantified by:

$$\phi_{BH} = \frac{1}{\sqrt{\dot{M}}} \int \mid B^r(r_{hor}) \mid dA_{\theta\phi}$$

- As time proceeds, the accumulated flux results in a magnetically arrested disk (MAD)
- Further accretion proceeds through other instabilities (esp. the interchange instability) developed in the plasma

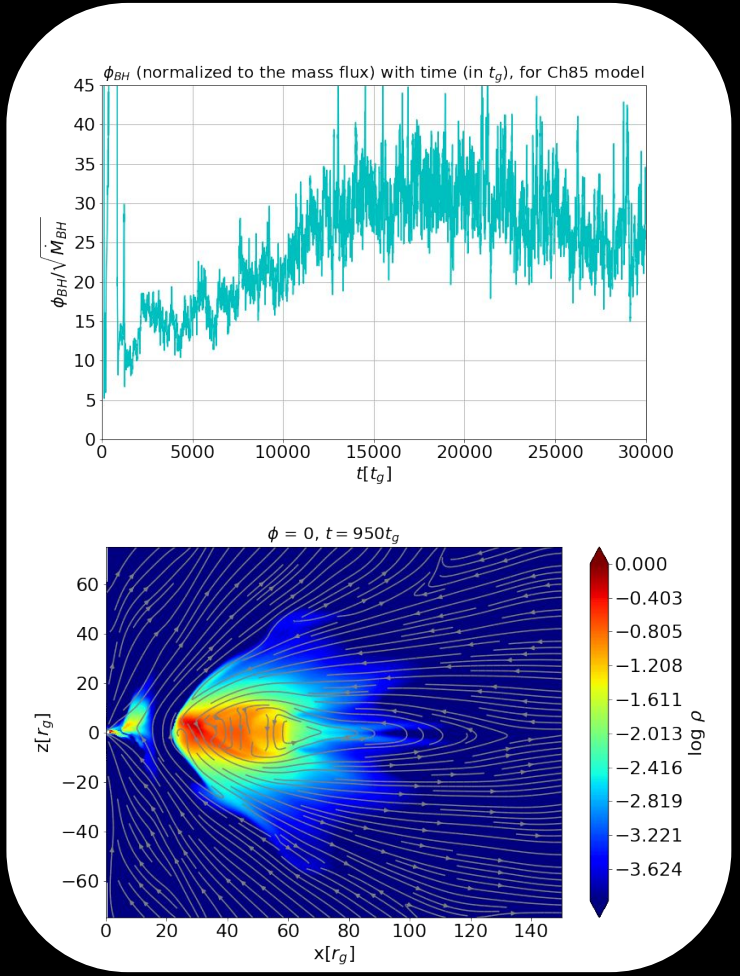

ϕ_{BH} with time (top panel) and a snapshot of the disk density structure along a poloidal slice (bottom panel)

Studying the Jet Variability

- We use the jet energy parameter

$$\mu = \frac{-T_t^r}{\rho u^r}$$

to study the variability of the jet emission. We can interpret this parameter as the total plasma energy flux normalized to the mass flux *(Sapountzis & Janiuk, 2019)*

- μ can provide an estimate of the maximum achievable Lorentz factor $\Gamma_\infty \sim \langle\mu\rangle_t$, assuming that all the Poynting and the thermal energy is transformed to baryon bulk kinetic *(Vlahakis & Königl, 2003; Sapountzis & Janiuk, 2019)*.
- We calculate μ at two chosen locations along the jet direction located at r = 150 r_g; θ = 5° (loc. 1) and θ = 10° (loc. 2) (averaged over φ) , to study the time variability of the jet.

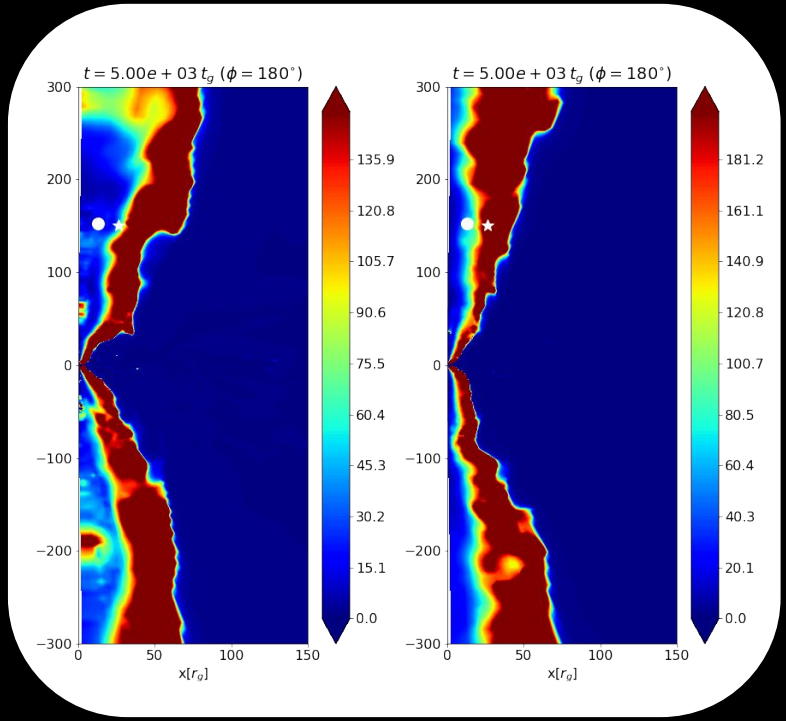

2D jet structure for the FM76 (left) and the Ch85 (right) models along a poloidal slice (ϕ = 180°) at an evolved time t = 5000 t_g with the marked points showing the locations 1 (dot) and 2 (star) where we measure the variability

Time Variability

- Minimum variability Time Scale (MTS) ~ peak widths at their half maximum on the μ-t plot

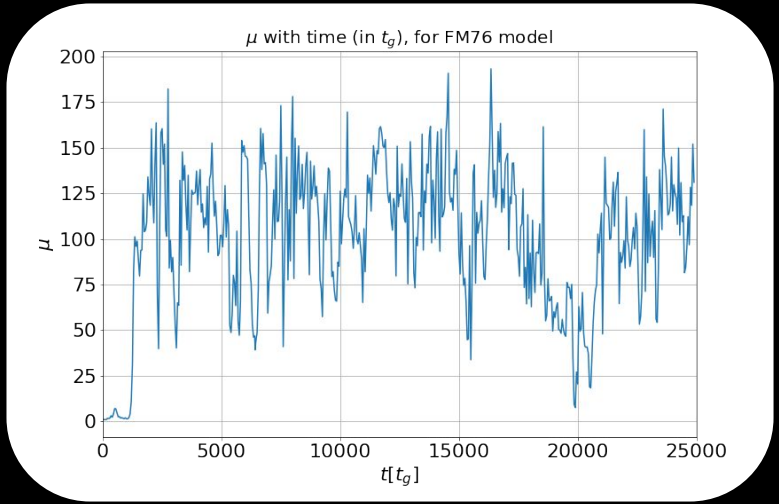

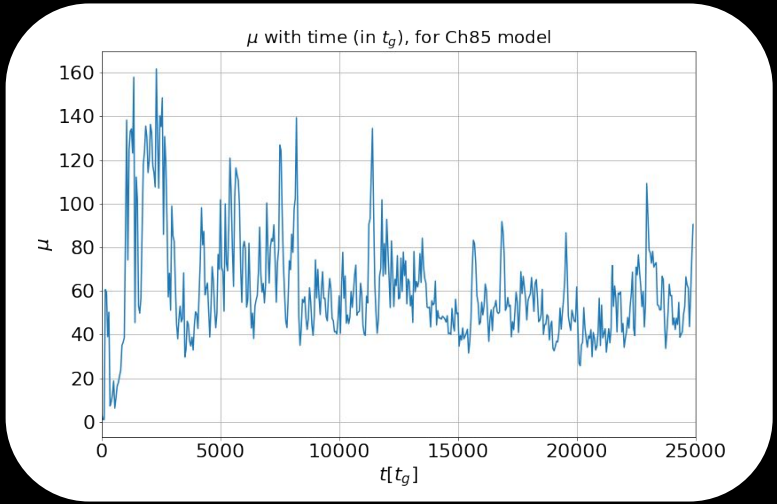

Variability of μ with time measured at the location 1 in the jet (r = 150 r_g; θ = 5°), and averaged over the toroidal angle φ

Time Variability

Model	Lorentz factor (Γ)			MTS estimated (in t_g)			Slope of the PDS	
	Loc. 1	Loc. 2	Average	Loc. 1	Loc. 2	Average	Loc. 1	Loc. 2
FM76	105.96	89.45	97.71	178.63	269.80	224.21	-0.8253	-1.4899
Ch85	61.33	202.36	131.85	147.01	147.72	147.37	-0.8016	-1.1310

- In physical units, the minimum variability timescale obtained for our **short-GRB (Ch85) model is 2.17 ms** and for the **long-GRB (FM76) model is 13.25 ms**. This matches with the range of observed values from a catalogue of GRB samples (MacLachlan et al. (2013)).
- The **slopes of PDS** at the chosen points also reveal information about the time variability. From the values, the outer wall of the jet shows higher variability when compared to the inner region of the jet closer to the axis. The slope values are in the lower range as compared to the values for the observed samples (Guidorzi et al. (2016), Dichiara et al. (2016), Dichiara et al. (2013)).

Jet Structure

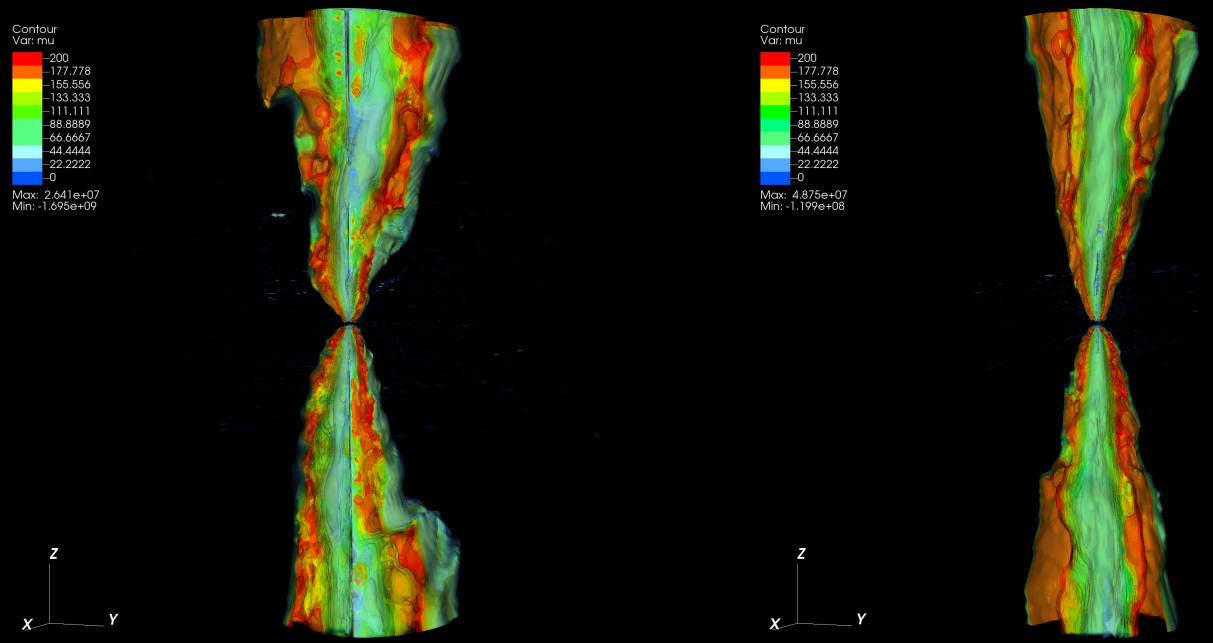

Jet structure at an evolved time t = 5000 t_g, resulting from the **FM76 model (left)** and the **Ch85 model (right)**. The plots show the contours of μ up to a radius of 200 r_g and clipped along the YZ-plane, show the structured nature of the jet with a relatively "hollow" core with higher Lorentz factors reached at the edges of the jet far away from the black hole rotation axis.

Jet Structure

- We compare our models with the observed short and long GRB jet structure and opening angles
- The jets from our models show structured outflows rather than a simple top hat
- The jets produced in our models have a hollow core up to angle ~ 5^o at their base and the higher Lorentz factors are reached at the outer edge of the jets, far from the rotation axis.
- We estimate the time averaged jet profile, at a large distance of 2000 r_g, with the polar angle to estimate the jet opening angles
- The jet in the long GRB (FM76) model has an opening angle ~ 11^o and in the short GRB (Ch85) model has an opening angle ~ 25^o

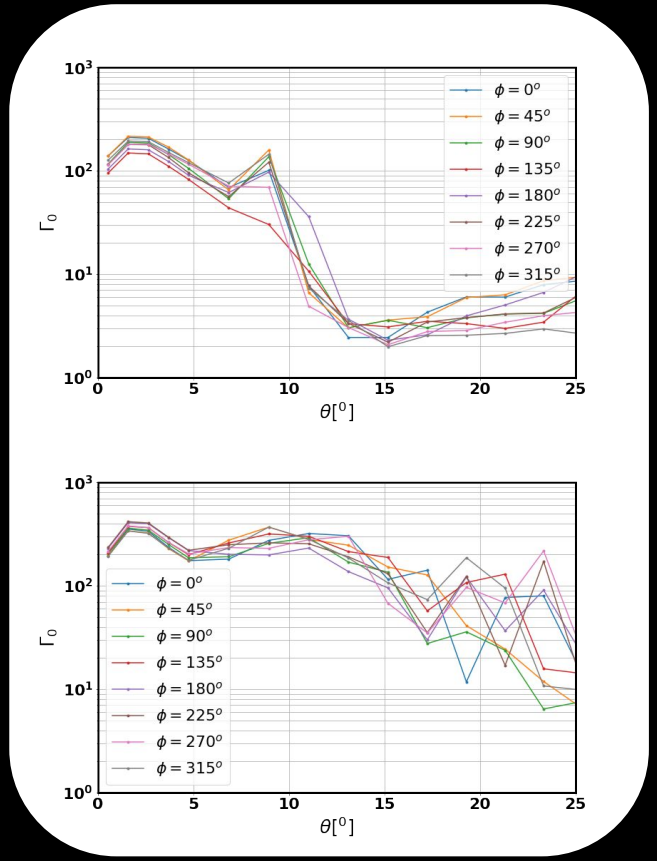

Time averaged jet Lorentz factor as a function of polar angle, measured at distance of 2000 r_g for the FM76 model, for long GRBs (top panel) and the Ch85 model, for short GRBs (bottom panel)

Summary

- We study the GRB **jet structure and temporal variability with a magnetically arrested disk** (MAD) state as the central engine
- Variability arises in the MAD models from unstable accretion flows mediated mainly by the **interchange instability** and/or magnetic reconnection (Ripperda et al. 2022). This can possibly explain episodic and intermittent jet behaviour.
- Our models produce jets with a hollow core up to an angle of 5^o at the base; they have an opening angle of up to ~ 25^o for the short-GRBs and up to ~ 11^o for the long-GRBs.
- **Structured jets** consistent with the recent observations. The opening angles we compute are in the range of observed values.
- The disk-jet interaction can result in **temporal variability down to a few ms scales**. The calculated MTS values are 2.17 ms for our short GRB model and 13.25 ms for our long GRB model.

Reference: *James, B., Janiuk, A., & Nouri, F. H., 2022, ApJ 935, 176*

Thank you!